Self-consistent kinetic modeling of low-pressure inductively coupled radio-frequency discharges

Yun Yang[a)] and Hanming Wu
Institute of Mechanics, Chinese Academy of Sciences, Beijing 100080, People's Republic of China

(Received 6 November 1995; accepted for publication 19 June 1996)

An efficient method for solving the spatially inhomogeneous Boltzmann equation in a two-term approximation for low-pressure inductively coupled plasmas has been developed. The electron distribution function (EDF), a function of total electron energy and two spatial coordinates, is found self-consistently with the static space-charge potential which is computed from a 2D fluid model, and the rf electric field profile which is calculated from the Maxwell equations. The EDF and the spatial distributions of the electron density, potential, temperature, ionization rate, and the inductive electric field are calculated and discussed. © *1996 American Institute of Physics.* [S0021-8979(96)09918-5]

I. INTRODUCTION

Recent applications of plasma in material processing, especially in the field of the semiconductor etching and deposition, have resulted in the introduction of a new generation of plasma sources operated at low pressures 1–100 mTorr.[1] Inductively coupled plasma (ICP), as one type of high-density plasma source, has been intensively studied both experimentally and theoretically. Modeling of those sources plays an important role in understanding the basic physical properties of the plasma and supports source design. For these low pressures, the spatially dependent description of the electron kinetics plays an important role. Since the electron energy relaxation length typically exceeds the characteristic discharge dimensions (of the order of 10 cm), the spatial diffusion of electrons is a much faster process than the diffusion in energy. Thus it has to be expected that the electron distribution function is governed by diffusive electron motion over whole discharge cross section, not just local characteristics.[2,3] Consequently the spatial displacement of the ionization rate with respect to the electric power deposition should be accounted for and the spatially inhomogeneous Boltzmann equation should be considered.

The intrinsically two-dimensional character of ICP that is sustained by an inductive rf electric field from a planar coil makes its modeling a rather complicated problem. A stable, relatively uniform high-density (10^{11}–10^{12} cm^{-3}) plasma can be created in a large volume.[4] Straightforward numerical simulation using Monte Carlo treatment of electrons is a computationally very demanding task.[5] The fluid model or some hydrodynamic approach,[6,19] which treats the electron gas as a fluid characterized by density, velocity, and mean energy, can give only a rather crude description of phenomena. Comparatively fast yet effective kinetic modeling of ICP has recently been developed by Kortshagen and Tsendin.[7] Their model self-consistently calculated the electron distribution function (EDF) and electric fields in the plasma, however, leaves out some important physics since it is assumed that all electrons are trapped in the plasma by a static space-charge electric field and imposed idealized boundary conditions.

A ''nonlocal approach'' which was proposed by Bernstein and Holstein[8] and Tsendin[9] relies on the fact that the energy relaxation length of the electrons greatly exceeds the momentum relaxation length and the dimensions of the discharge chamber are typically less than or comparable to the energy relaxation length. The key idea of this approach consists of the assumption that the trapped electron kinetics can be described by a distribution function of total electron energy (i.e., kinetic plus potential energy) which is determined from a spatially averaged kinetic equation. This idea proved to be effective in application to various gas discharge problems[10–13] and has recently been applied to ICP modeling.[7,14] The experimental data[13,14] demonstrate that for the majority of electrons the EDF is a function of total electron energy only and does not depend explicitly on the coordinates. However, a relatively small fraction of electrons in an ICP cannot be treated using the spatially averaged kinetic equation as indicated by Kolobov and Hitchon.[15] These are free electrons which are capable of escaping to the chamber walls and fast electrons having an energy relaxation length less than the discharge dimensions. These electrons give small contributions to the plasma density but determine such important discharge characteristics as electron direct current density and the ionization rate.

The present article is devoted to the kinetic treatment of electrons in ICP and self-consistent simulation of collisional ICP. The model is based on calculation of the electron distribution function (EDF) via solution of a spatially inhomogeneous Boltzmann equation coupled with a self-consistent solution of the ion continuity equation and electromagnetic equations for the rf field.

II. ELECTRON BOLTZMANN EQUATION FOR ICP

We consider an ICP driven by the electric field from a spiral coil placed on the dielectric roof of a cylinder with metallic walls and bottom [Fig. 1(b)]. The plasma is generated and heated by an inductively coupled azimuthal electric field E. A space-charge field is built up which assists the ion current and retards the dc electron current. In the plasma, a

[a)]Electronic mail: hmw@cc5.imech.ac.cn

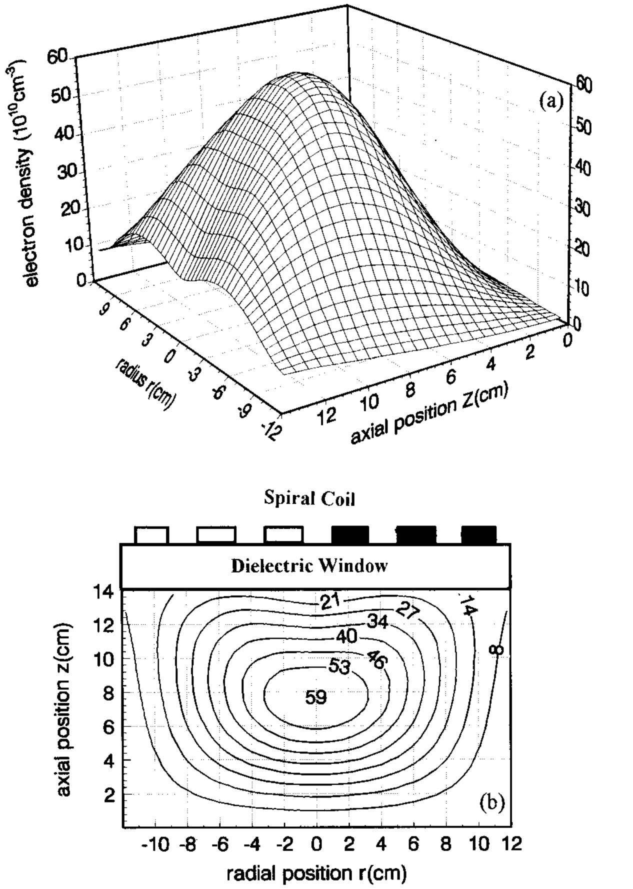

FIG. 1. Profile of electron density (a) and schematic of the discharge and contours of electron density (b) for Argon pressure 20 mTorr and power 500 W.

weak ambipolar space-charge field give rise to a combination of diffusive and mobility flow of charged particles. In addition, a potential drop in the sheath is set up to trap the majority of the electrons and balance the total electron and ion currents to the walls. For typical pressures, the electron energy relaxation length exceeds the discharge dimensions. Thus, it is useful to include the influence of the static field on the electron kinetics using the total energy of the electrons $\epsilon = w - e\phi(z,r)$, where w is kinetic energy of electrons.[8–10] Since the change of the total energy due to the electron heating by the rf field and energy transfer in collisions are slow compared to the time scale of the spatial displacement of electrons, the total energy ϵ is approximate invariant of the electron motion.

The Boltzmann equation is simplified by using conventional two-term approximation:

$$f = f_0(\epsilon,z,r) + \boldsymbol{\nu}/\nu \cdot \mathbf{f}_1(\epsilon,z,r,t), \tag{1}$$

where $f_1 \ll f_0$. For the rf field $E_\theta(z,r,t) = E_0(z,r)e^{j\omega t}$, the anisotropic part $\mathbf{f}_1$ breaks into oscillatory and steady-state parts:

$$\mathbf{f}_1 = \mathbf{f}_1^0(\nu,z,r) + \mathbf{f}_1^1(\nu,z,r)\exp(j\omega t). \tag{2}$$

Bearing in mind the above assumptions and using the total energy ϵ as an independent variable, the kinetic equation can be written in the form:[8–10,14]

$$\frac{1}{r}\frac{\partial}{\partial r}\left[r\nu D_r(z,r,\epsilon)\frac{\partial f_0}{\partial r}\right] + \frac{\partial}{\partial z}\left[\nu D_r(z,r,\epsilon)\frac{\partial f_0}{\partial z}\right] + \frac{\partial}{\partial \epsilon}\left[\nu D_\epsilon(z,r,\epsilon)\frac{\partial f_0}{\partial \epsilon}\right] = \sum_k \left[\nu \upsilon_k^*(w) f_0 - \sqrt{\nu^2 + \frac{2\epsilon_k^*}{m}} \times \upsilon_k^*(w+\epsilon_k^*) f_0(\epsilon+\epsilon_k^*)\right] + J_{\mathrm{el}} + J_{\mathrm{ee}}, \tag{3}$$

$$\mathbf{f}_1^0 = -\frac{\nu}{\upsilon_m}\,\mathrm{grad}\, f_0, \tag{4}$$

$$\mathbf{f}_1^1 = -\frac{\nu e \mathbf{E}_\theta}{\upsilon_m + i\omega}\frac{\partial f_0}{\partial \epsilon}, \tag{5}$$

where $D_r = \nu^2/3\upsilon_m$ and $D_\epsilon = [e^2E_0^2(z,r)\nu^2\upsilon_m]/6(\upsilon_m^2+\omega^2)$ are the diffusion coefficients in space and energy, respectively. υ_m and υ_k^* are the momentum transfer and inelastic collision frequencies ($\upsilon_m \gg \upsilon_k^*$). The first term on the right-hand side of Eq. (3) representing the electrons which have suffered inelastic collisions is written for the simplest case of the excitation of level k with energy ϵ_k^*. The last two terms J_{el} and J_{ee} on the right-hand side of Eq. (3) are the collision integrals for elastic, and electron-electron interactions, respectively. The time-averaged energy gain from the rf field corresponds to diffusion in ϵ. The energy diffusion coefficient D_ϵ decrease rapidly with distance from the coil. The heating is therefore spatially inhomogeneous and occurs mainly in the vicinity of the coil.

The spatially dependent kinetic Eq. (3) represents an elliptic partial differential equation which can be solved numerically. The boundary conditions are important for the solution of this equation. The domain of integration is not rectangular but possesses an irregular boundary defined by the space potential $\epsilon = -e\phi(z,r)$ where the kinetic energy is zero, i.e., $w(z,r)=0$. At each boundary a boundary condition has to be specified. We take the boundary condition as follows:[15,16]

$$\left.\frac{\partial f_0}{\partial r}\right|_{r=0} = 0, \tag{6a}$$

$$\left.\frac{\partial f_0}{\partial \eta}\right|_{\epsilon \leqslant -e\phi_w} = 0, \quad -D_r\left.\frac{\partial f_0}{\partial \eta}\right|_{\epsilon > -e\phi_w} = \nu f_0 \frac{\Omega}{4\pi}, \tag{6b}$$

$$f_0|_{\epsilon\to\infty} = 0, \tag{6c}$$

$$-\frac{\partial \phi(z,r)}{\partial r} D_r \left.\frac{\partial f_0}{\partial r}\right|_{w=0} - \frac{\partial \phi(z,r)}{\partial z} D_r \left.\frac{\partial f_0}{\partial z}\right|_{w=0} = D_\epsilon \left.\frac{\partial f_0}{\partial \epsilon}\right|_{w=0}. \tag{6d}$$

Equation (6a) is the boundary condition on the discharge axis following from the rotational symmetry. The first equation in condition (6b), where η denotes the direction normal to the wall and ϕ_w is the potential of the wall, is the boundary condition for trapped electrons corresponding to their reflection by the potential wall and the second equation expresses the boundary condition at $\epsilon > -e\phi_w$ that obtained by imposing equality of the normal component of the electron diffusive flux and the electron loss to the wall.[15,16] The solid angle Ω of the loss cone is given by

$$\Omega = 2\pi[1 - \sqrt{e\Delta\phi/(\epsilon + e\phi_{\mathrm{sh}})}], \tag{7}$$

where $\Delta\phi$ is the potential drop in the sheath near the wall. The electrons having kinetic energy $w = \epsilon + e\phi_{\mathrm{sh}}$ after last scattering can overcome the potential drop $\Delta\phi$ and reach the absorbing wall. The condition (6d) is deduced from the validity of Eq. (3) on the boundary $w=0$. By considering the physical processes occurring at this boundary that there is neither a source nor a sink of electrons along this boundary and requiring the divergence of a diffusive flux perpendicular to that boundary between the spatial and energy space must be continuous.[16]

III. ELECTROMAGNETIC EQUATIONS

The electromagnetic field in ICP reactor can be primary divided in two parts: the inductively coupled electromagnetic field $\mathbf{E}_I$ and electrostatic field $\mathbf{E}_S$. Their resultant can be written as $\mathbf{E} = \mathbf{E}_I + \mathbf{E}_S$, where $\mathbf{E}_S = -\nabla\phi$, ϕ is the static electric potential.

The inductive field $\mathbf{E}_I$ has the azimuthal component E_θ only. The oscillating current in the coil $I = I_0 \cos \omega t$ produces inductive electric field $E_\theta \propto \exp(j\omega t)$. The E_θ component satisfy equation (see the Appendix):

$$\frac{1}{r}\frac{\partial}{\partial r}\left(r\,\frac{\partial E_\theta}{\partial r}\right) + \frac{\partial^2 E_\theta}{\partial z^2} - \frac{1}{r^2}\,E_\theta + \left(\frac{\omega}{c}\right)^2 E_\theta = j\omega\mu_0\sigma_e E_\theta, \tag{8}$$

where $\mu_0 = 4\pi\times 10^{-7}$ H/m, σ_e is the plasma electric conductivity can be derived from EDF as

$$\sigma_e(z,r) = -\frac{2e^2}{3m}\int_{-e\phi}^{\infty}\frac{1}{\upsilon_m + j\omega}\,\frac{\partial f_0}{\partial \epsilon}\,(\epsilon + e\phi)^{3/2}d\epsilon. \tag{9}$$

For the ICP reactor as shown in Fig. 1, on the metallic chamber wall and the reactor axis, $E_\theta = 0$, while on the top surface, E_θ is determined by the current I_0 in the coil and the inductive current in the plasma.[17–19]

IV. FLUID DYNAMIC MODEL

Due to the great importance of the space-charge potential, it is a further task to determine the potential profile $\phi(z,r)$. We constitute it via fluid model for ions as it did by Ref. 23. The time average equations for the ion is[6,19]

$$\nabla\cdot\mathbf{J}_i = R_i, \tag{10}$$

where $\mathbf{J}_i = -\mu_i n_i \nabla\phi(z,r) - (k\mu_i/e)\nabla(n_i T_i)$, k is Boltzmann constant, μ_i, n_i, and T_i is the mobility, density, and temperature of ion, respectively. Assuming quasi-neutrality condition and neglecting the thermal energy of ions in comparison to that of the electrons as well as their inertia, we rewrite Eq. (10) as

$$\nabla\cdot[\mu_i n_i \nabla\phi(z,r)] = -R_i. \tag{11}$$

n_i which is equal to n_e of electron density can be deduced from EDF:

$$n_i(z,r) = n_e(z,r) = \int_{-e\phi(z,r)}^{\infty} f_0(z,r,\epsilon)\sqrt{\epsilon + e\phi(z,r)}\,d\epsilon. \tag{12}$$

The ionization rate R_i can be given by

$$R_i(z,r) = \int_{u_i - e\phi(z,r)}^{\infty}\sqrt{\epsilon + e\phi(z,r)}\times\upsilon_i[\epsilon + e\phi(z,r)]f_0(z,r,\epsilon)\,d\epsilon, \tag{13}$$

where u_i and υ_i are the ionization threshold and frequency.

The solution of Eq. (11) results in a potential profile in the plasma as it was done by Kortshagen *et al.*[23] The Bohm criterion, that the potential drop in the plasma over the last ion mean-free path before the wall has to be equal to $kT_e'/2e$, should be fulfilled in front of all walls, i.e.,

$$e|\nabla\phi(z,r)|_\eta \lambda_i = \frac{kT_e'}{2}, \tag{14}$$

where η denotes the direction normal to the wall and λ_i is the ion mean-free path. The electron temperature T_e', which appears in the ion sound speed, is defined as screening temperature.[23] Because of the symmetry, the boundary condition on the axis leads to

$$\left.\frac{\partial\phi(z,r)}{\partial r}\right|_{r=0} = 0. \tag{15}$$

With the boundary condition (14), (15), the solution of Eq. (11) results in a potential profile at plasma-sheath boundary, but the wall potential ϕ_w should be defined. In the case of metal walls, the value of ϕ_w is constant over the whole wall surface. The wall potential ϕ_w is calculated from the balance of electron and ion fluxes to the wall and from the equality of the total volume ionization and the number of electrons escaping to the wall. The total number of inelastic collisions and electron escapes to walls per unit time can be found from Eq. (3) by integrating that equation over the space and over the energy of electrons capable of reaching the wall. Following Kolobov *et al.*[24] we have

$$\left(1 + \frac{1}{g}\right)\int_S \nu D_\epsilon \left.\frac{\partial f_0}{\partial \epsilon}\right|_{e\phi_w} r\;dr\;dz = \int_S \nu D_\epsilon \left.\frac{\partial f_0}{\partial \epsilon}\right|_{\epsilon *} r\;dr\;dz, \tag{16}$$

which defines the wall potential, with S the available discharge area boundary. The wall potential was calculated from Eq. (16) for the efficiency of stepwise ionization $g = 1/3$.

The electron temperature T_e, which is defined as mean electron energy, can be deduced from EDF:

$$T_e = \frac{2}{3n_e}\int_{-e\phi(z,r)}^{\infty} f_0(z,r,\epsilon)[\epsilon + e\phi(z,r)]^{3/2}d\epsilon. \tag{17}$$

V. RESULTS AND DISCUSSIONS

The numerical treatment comprises a number of tasks which have to be solved self-consistently. A starting poten-

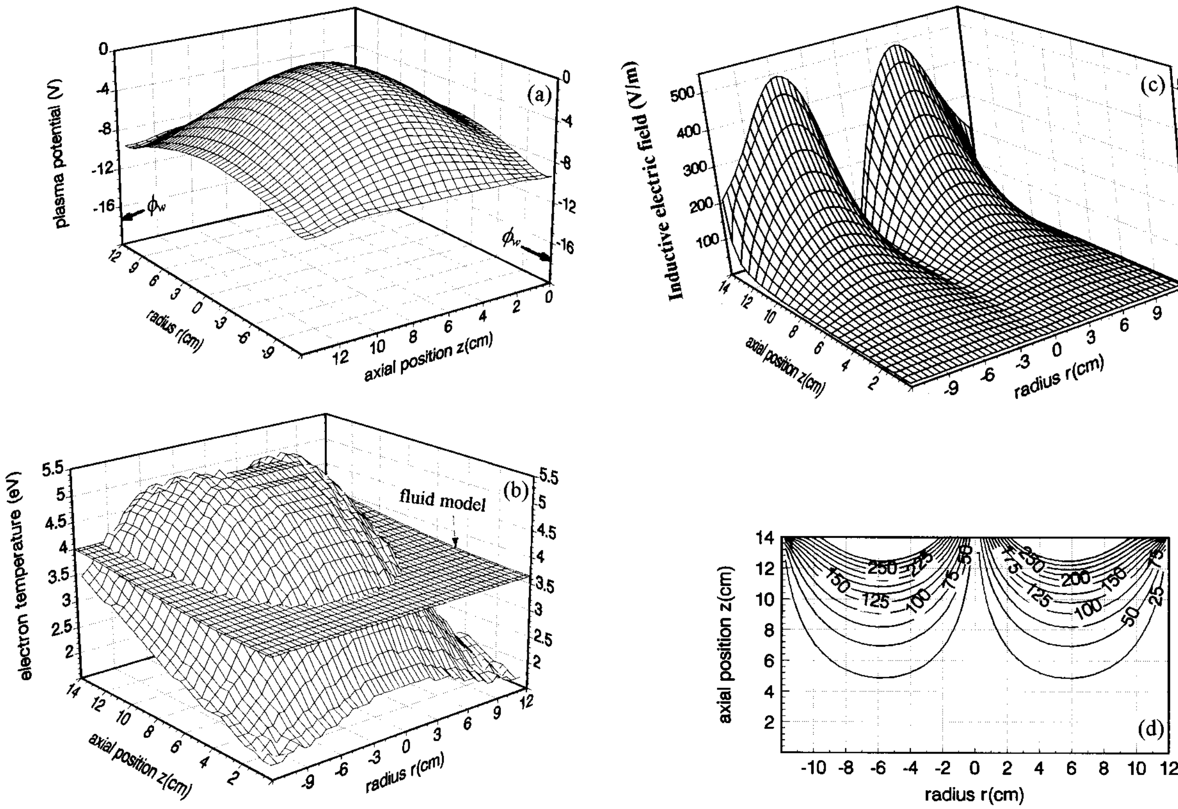

FIG. 2. Profiles of the static space charge potential, ϕ_w (-17.3 V) denotes the wall potential (a), electron temperature (mean electron energy) and the result of fluid model (b), rf inductive field (c) and contours of rf inductive field (d), for Argon pressure 20 mTorr and power 500 W.

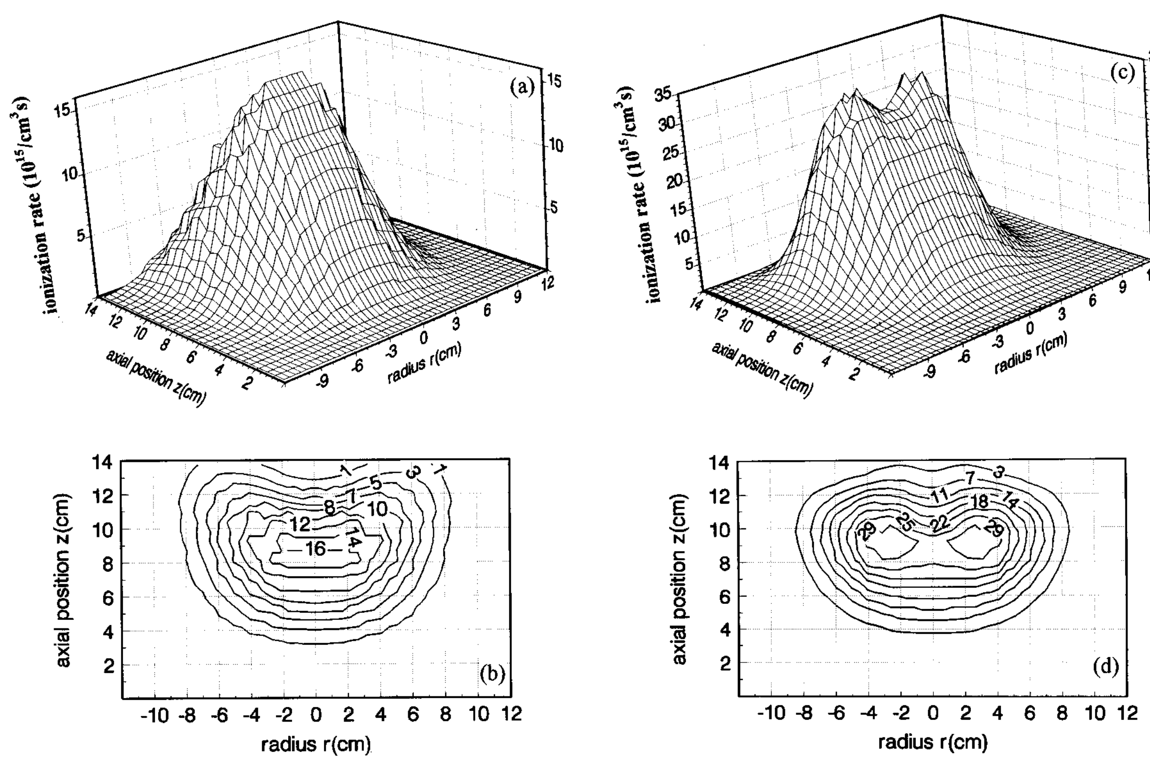

FIG. 3. Ionization rate profiles and contours for Argon pressure 20 mTorr (a), (b) and 40 mTorr (c), (d) with power 500 W.

tial was assumed, which for simplicity was chosen as a parabolic potential. With this starting potential and some starting value the spatial dependent EDF can be evaluated from Eq. (3) using some standard iterative method. Then the azimuthal component of rf electric field was calculated from Eq. (8) for a given coil current. A new potential and wall potential ϕ_w was calculated from the solution of Eqs. (11) and (16). Temperature of electrons was deduced from the solution of Eq. (17). Electron density was calculated from Eq. (12). With this new potential the procedure restarts iteratively. Equations (3), (8), and (11) are discretized on grids 28 times 28 in space and 50 points in the energy, and solved via a multigrid algorithm. Typical computation times about 4 h on a usual personal computer (PC 586-processor, 100 MHz) are achieved.

The typical profiles for plasma density n_e, electron temperature T_e, plasma potential ϕ, the azimuthal electric field intensity E_θ, and the ionization rate R_i are shown in Figs. 1, 2, and 3. The total input power is 500 W with 20 mTorr neutral pressure. The electron density get its maximum in the vicinity of the center (Fig. 1). The electrons are confined by the space charge potential [Fig. 2(a)] and most of them are trapped in the center. The electron temperature (mean electron energy) has its maximum (about 5.25 eV) in the vicinity of coil and drops gradually to the bottom and wall [Fig. 2(b)]. These results seem quite close to those obtained by experiment[20] and by the non-local simulation.[7] Compared with the results of fluid model[19] shown in Fig. 2(b), the mean energy of the electrons is more spatially nonuniform due to high thermal conductivity of electrons. In fluid model, the electron temperature is very smooth.

The inductive electric field [Figs. 2(c), 2(d)] decreases rapidly from the roof to the bulk plasma due to the finite skin depth (about 1–2 cm for $10^{11}-10^{12}$ cm^{-3} plasma density). The wall potential ϕ_w, bulk electron temperature T_e, and maximum electron density n_e are about -17.3 V, 4.3 eV, and 5.9×10^{11} cm^{-3}, respectively, which are quite close to the experimental results.[21]

Figure 3 shows the calculated spatial distribution of the excitation rate which have the same features as in Ref. 15 and 21. When the pressure decreases, the maximum of excitation rate moves from off axis and peaks near the center of the discharge where the rf field is absent. As discussed by Kolobov and Hitchon,[15] nonlocal approach helps us to explain the difference between the experimentally observed shapes of the light emission for different pressures. When the pressure increases, the electron energy relaxation length becomes less than the discharge dimensions and the fast electrons undergo inelastic collisions before reaching the region of the highest potential.

In order to get an impression of the influence of the spatial inhomogeneity, in Fig. 4 EDFs of total energy are presented as a function of the radius in radial position ($Z=5$ cm) and in axial direction from the dielectric on the axis. Note that the boundary of the curve corresponds to the boundary $\epsilon=-e\phi(z,r)$ or $w(z,r)=0$. These surfaces exactly represent onsets of the EDFs of kinetic energy in different radial and axial positions. The EDF reveal small deviations from spatial homogeneity, especially in the EDF tail where

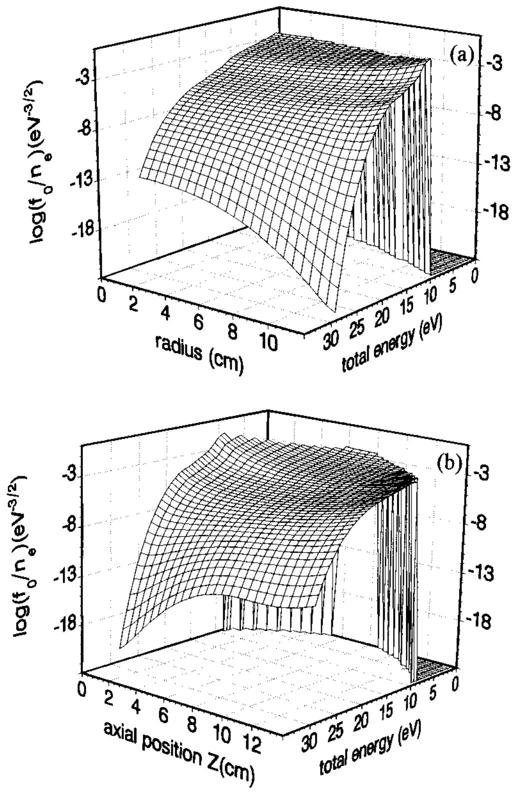

FIG. 4. Normalized EDF by solution of the spatially inhomogeneous kinetic equation: in radial direction ($z=5$ cm) (a) and in axial direction from the dielectric on axis (b) for Argon pressure 20 mTorr and power 500 W.

inelastic collisions occur. Depletion of the EDF tail is observed in the highest potential region, especially in the center region of the discharge. For a given total energy, the kinetic energy is maximal in the center and thus also the efficiency of inelastic collisions. The EDF near the coil have an enhanced tail due to the rf heating. Near the wall the tail is depleted due to electron escaped to wall as indicated by Kolobov *et al.*[24]

In Fig. 5, the axial and radial distribution of the EDF are shown which have the same features as those measured in the experiment.[14] It is seen that to good accuracy the EDF coincide with each other in the elastic energy range where the EDF does not depend explicitly on coordinates. In the inelastic energy range, especially the EDF of free electron, the EDF drops rapidly due to inelastic collisions and does depend on the coordinates.

The main conclusions of the present work are as follows: An example of strict solution of the spatial inhomogeneous Boltzmann's equation for electrons in two spatial dimensional for a low-pressure inductively coupled rf discharge is presented. The EDF in present model is found self-consistently with the electromagnetic fields. The electron kinetics is coupled with a self-consistent solution of ion continuity equation and equations for rf field. The EDF is found as a function of total energy and two spatial coordinates. To good accuracy, the EDF of trapped electrons does not depend explicitly on the coordinates. Spatial distributions of electron density, temperature, ionization rate, inductive field, and plasma potential are obtained. The effect of the gas pres-

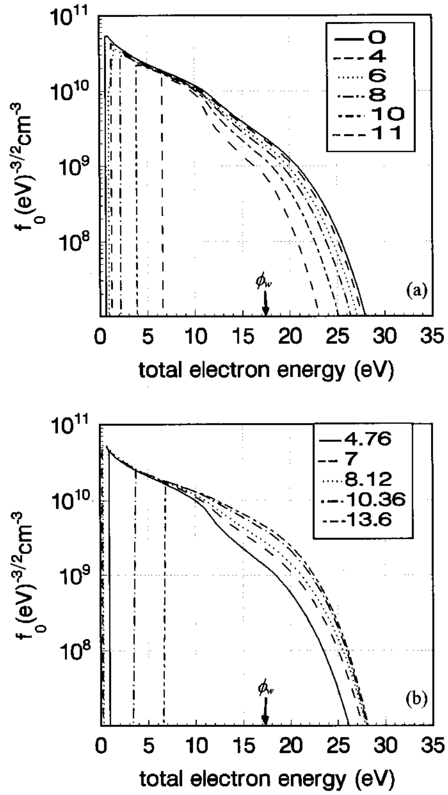

FIG. 5. The axial and radial evolution of the EDF. Labels correspond to radial distance from the center at a fixed axial distance (4.4 cm) from the dielectric window (a) and axial distance from the dielectric on axis (b) for Argon pressure 20 mTorr and power 500 W. ϕ_w (17.3 V) denotes the wall potential.

sure and quantitative comparison with the experimental data will be given elsewhere.

ACKNOWLEDGMENTS

This project was supported by the Science Foundation of the Chinese Academy of Sciences. The authors are grateful for the referees' instructive comments and thank Z. Sun for help with some of the numerical calculations and also thank W. N. G. Hitchon and V. I. Kolobov for providing copies of their work prior to publication.

APPENDIX: DERIVATION OF THE EQUATION FOR E_I

From Faraday's law and Ampere's law (in vacuum), it can be shown that

$$-\nabla\times\nabla\times\mathbf{E}=\mu_0\frac{\partial}{\partial t}\left(\mathbf{J}+\epsilon_0\frac{\partial\mathbf{E}}{\partial t}\right). \tag{A1}$$

Here we only consider the region interior to the plasma, no external coil currents are included in **J**. Assuming azimuthal symmetry, the rf field and current density **E** and **J** only have azimuthal componts: E_θ and J_θ. Equation (A1) becomes

$$\frac{1}{r}\frac{\partial}{\partial r}\left(r\frac{\partial E_\theta}{\partial r}\right)+\frac{\partial^2 E_\theta}{\partial z^2}-\frac{1}{r^2}E_\theta=\mu_0\frac{\partial J_\theta}{\partial t}+\frac{1}{c^2}\frac{\partial^2 E_\theta}{\partial t^2}. \tag{A2}$$

Now express the current as $J_\theta=-en_eu_\theta$, where u_θ and n_e are the electron velocity (azimuthal) and density. Assuming that E_θ, $u_\theta\propto\exp(j\omega t)$, Eq. (A2) becomes

$$\frac{1}{r}\frac{\partial}{\partial r}\left(r\frac{\partial E_\theta}{\partial r}\right)+\frac{\partial^2 E_\theta}{\partial z^2}-\frac{1}{r^2}E_\theta+\left(\frac{\omega}{c}\right)^2E_\theta =-j\omega\mu_0en_eu_\theta. \tag{A3}$$

For simple case, the azimuthal electron velocity and electric field satisfy the momentum equation,

$$m\frac{\partial u_\theta}{\partial t}=-eE_\theta-m\upsilon_mu_\theta, \tag{A4}$$

where m and υ_m are the electron mass and collison frequency for momentum transfer. By assuming $u_\theta\propto\exp(j\omega t)$, Eq. (A4) yields,

$$u_\theta=\frac{e}{m}\frac{1}{\upsilon_m+j\omega}E_\theta=\mu_eE_\theta, \tag{A5}$$

where μ_e is the electron mobility transport coefficient. For the sake of generality, in the absence of a magnetic field, the mobility μ_e can be written by EDF as:[22]

$$\mu_e=\frac{e}{n_em}\int\frac{1}{\upsilon_m+j\omega}\frac{4\pi\nu^3}{3}\frac{\partial f_0}{\partial\nu}d\nu, \tag{A6}$$

where ν is the electron velocity. Enter Eqs. (A5), (A6) into (A3), and let $\sigma_e=n_ee\mu_e$ we can finally get Eq. (8).

[1] M. A. Lieberman and R. A. Gottscho, in *Physics of Thin Films*, edited by M. Francombe and J. Vossen (Academic, New York, 1994), Vol. 18, pp.1–119.
[2] U. Kortshagen, J. Phys. D **26**, 1691 (1993).
[3] V. A. Godyak and R. B. Piejak, Appl. Phys. Lett. **63**, 3137 (1993).
[4] M. S. Barnes, J. C. Forster, and J. H. Keller, Appl. Phys. Lett. **62**, 2622 (1993)
[5] P. L. G. Ventzek, R. J. Hoekstra, and M. J. Kushner, J. Vac. Sci. Technol. B **12**, 461 (1994).
[6] R. A. Stewart, P. Vitello, and D. B. Graves, J. Vac. Sci. Technol. B **12**, 478 (1994).
[7] U. Kortshagen and L. D. Tsendin, Appl. Phys. Lett. **65**, 1355 (1994).
[8] I. B. Bernstein and T. Holstein, Phys. Rev. **94**, 1475 (1954).
[9] L. D. Tsendin, Sov. Phys. JETP **39**, 805 (1974).
[10] I. D. Kaganovich and L. D. Tsendin, IEEE Trans. Plasma Sci. **PS-20**, 66 (1992).
[11] V. I. Kolobov and L. D. Tsendin, Phys. Rev. A **46**, 7837 (1992).
[12] U. Kortshagen, Phys. Rev. E **49**, 4369 (1994).
[13] U. Kortshagen, I. Pukropski, and M. Zethoff, J. Appl. Phys. **76**, 2048 (1994).
[14] V. I. Kolobov, D. F. Beale, L. J. Mahoney, and A. E. Wendt, Appl. Phys. Lett. **65**, 537 (1994).
[15] V. I. Kolobov and W. N. Hitchon, Phys. Rev. E **52**, 972 (1995).
[16] C. Bush and U. Kortshagen, Phys. Rev. E **51**, 280 (1995).
[17] X. Chen and E. Pfender, Plasma Chem. Plasma Process. **11**, 103 (1991).
[18] B. W. Yu and S. L. Girschick, J. Appl. Phys. **69**, 656 (1991).
[19] M. Li, H. M. Wu, and Y. M. Chen, IEEE Trans. Plasma Sci. **23**, 558 (1995)
[20] J. Hopwood, C. R. Guarnieri, S. J. Whitehair, and J. J. Cuomo, J. Vac. Sci. Technol. A **11**, 152 (1993).
[21] L. J. Mahoney, A. E. Wendt, E. Barrios, C. J. Richards, and J. L. Shohet, J. Appl. Phys. **74**, 2041 (1994).
[22] I. P. Shkarofsky, T. W. Johnston, and M. P. Bachynski, *The Particle Kinetics of Plasma* (Addison–Wesley, Reading, MA, 1966).
[23] U. Kortshagen, I. Pukropski, and L. D. Tsendin, Phys. Rev. E **51**, 6063 (1995).
[24] V. I. Kolobov, G. J. Parker, and W. N. G. Hitchon, Phys. Rev. E **53**, 53 (1996).